

# GAUSSIAN MIXTURES FOR INTENSITY MODELING OF SPOTS IN MICROSCOPY

Kangyu Pan, Anil Kokaram

Trinity College Dublin  
Department of Electronic and Electrical Engineering  
Dublin-2, Ireland

Jens Hillebrand, Mani Ramaswami

Trinity College Dublin  
Institute for Neuroscience  
Dublin-2, Ireland

## ABSTRACT

In confocal microscopy imaging, the target objects are labeled with fluorescent markers in the living specimen, and usually appear as spots in the observed images. Spot detection and analysis is an important task for the biological studies from the observed images. However, while the spots have irregular sizes and positions due to the variant amount of objects on each spot, the quantitative interpretation of the labeled objects is still heavily reliant on manual evaluation. In this paper, a novel shape modeling algorithm is proposed for automating the detection and analysis of the spots of interest. The algorithm exploits a Gaussian mixture model to characterize the spatial intensity distribution of the spots, and optimizes the model parameters using split-and-merge expectation maximization (SMEM) algorithm. As a result, a large amount of target objects with uncertain shapes can be analyzed in a systematic way.

**Index Terms**— Gaussian mixture model, split-and-merge EM algorithm, spot analysis, mRNA, shape modeling

## 1. INTRODUCTION

Formation of long term memory requires new protein synthesis at specific synapses. To regulate mRNA translations, mRNAs have to be repressed, transported to synapses and activated on neuronal stimulation. The distribution of proteins involved in these processes is of immediate interest in research on memory formation. In this paper we are specifically interested in *Drosophila* homology Me31B. To further investigate the role of Me31B in neuronal translation, we investigate the co-localization of Me31B with other proteins of interest. To this end, different proteins are labeled by immunostainings with different fluorescent markers in a living specimen, and a fluorescent image of each type of protein is captured by confocal microscopy. Co-localization analysis of different specific proteins then implies detection and isolation of each protein particle in each image. As particles visually manifest as spots, the problem is to detect and quantify the shapes and positions of spots in each image. Several automated spot analysis systems in fluorescence microscopy have been developed

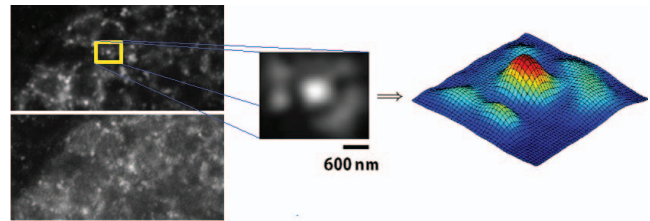


**Fig. 1.** Spot images and an example profile. *Left image shows two different staining of the same tissue location (top and bottom).*

that apply different tools [1], e.g. wavelet multiscale products [2], multiscale variance-stabilizing transform [3], Haar feature based Adaboost algorithm [4] and  $h$ -dome transformation [5] based on the presence of regular, separated spots in relatively uncluttered background. However, in our work, images exhibit brightness and noise variation as well as clustered particles and hence spot appearance is widely varying. Thus existing techniques are unable to estimate the positions of protein particles in a given spot. The key to resolving the problem is to observe that the intensity profile  $I(\vec{x})$  of a single protein particle, as shown in Fig.1, bears some resemblance to a 2D Gaussian distribution. It is therefore sensible to characterize each spot as a Gaussian mixture model where each protein particle is modeled by a weighted mixture component  $N(\vec{x}|\vec{\mu}_n, \Sigma_n)$  with mean  $\vec{\mu}_n$  and covariance  $\Sigma_n$  as follows.

$$I(\vec{x}) = \sum_{n=1}^N \alpha_n N(\vec{x}|\vec{\mu}_n, \Sigma_n)$$

Where  $\alpha$  is the mixing weight and  $\sum_{n=1}^N \alpha_n = 1$ . Well established EM algorithms exist for mixture component estimation, but they need to be adapted before they are suitable in this case. The novel step in shape modeling in this paper is to map the probability of a variable  $x$  in the EM algorithm to the surface brightness of a spot-region at pixel site  $(h, k)$ , because in this case the ‘distribution’ to be modeled is known and equivalent to the spot appearance itself.

The proposed algorithm has three stages: 1) Pre-processing operation for detecting and separating the spots of interest from the original image; 2) fitting a Gaussian mixture model to each isolated spot of the two fluorescent images using a split-and-merge expectation-maximization (SMEM)

algorithm and finally 3) using the estimated parameters to represent the geometric characteristics of the corresponding particles and hence deriving measures of co-localization.

## 2. PRE-PROCESSING

The observed image is assumed to be the result of blurring a true, original image with a point-spread function (PSF) and corrupted with additive noise. In the first step, the raw image is denoised and deblurred by deconvolution with a  $7 \times 7$  disk kernel. A canned Matlab routine is used. In the second step, spots of interest are detected. However, as shown in Fig.2, the background brightness in the fluorescent image is inhomogeneous. In order to identify the spots without the background bias, the second step exploits a modified contrast method.

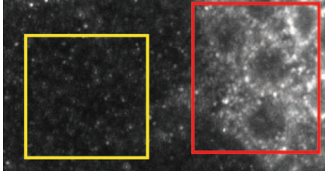


**Fig. 2.** Irregular background brightness problem (Two regions are shown that the background have extremely variable brightness.)

**Spot extraction:** The positions of spots are detected as regions of high contrast in the image. Contrast  $\psi(\cdot)$  is measured using the work of Boudraa *et al.* [6] and then modified slightly with a gamma operation to improve spot detectability. Hence  $I_c(\cdot) = [\psi(I(\cdot))]^\alpha$ , where  $I_c(\cdot)$  is the gamma corrected intensity image. Fig.3 illustrates that the idea of  $I_c(\cdot)$  is reducing the different spot intensities caused by irregular background brightness and emphasize the edges of the spots. The positions of spots are then detected by thresholding  $I_c(\cdot)$  with a user defined value (where it is 3 in our experiment, Fig.3). The thresholded patches are raw spot regions and typically underestimate the extent of each spot. To detect the entire region, each detected spot patch is extended to the boundaries defined by the nearest zero-crossing (in the gradient image using difference of Gaussians, DoG) to the spot peak.

**Background subtraction:** In order to model the actual shape of the spot, the extracted spot is normalized by subtracting the local background. Thus the last step of pre-processing is background subtraction. As shown in Fig.2, background brightness varies smoothly over a much larger area compared to a spot. The local background is then reasonably considered to be a flat plane which is shown in Fig.5. The estimation of the background ( $B(\cdot)$ ) uses the least square error method to fit a plane to the boundary pixels of the spot region.

## 3. SHAPE MODELING

Given normalized patches from pre-processing, a Gaussian mixture model is used to model the intensity profile of each spot. This is a difficult optimization process, i.e. to select both the number  $M$  of Gaussian components and their parameters

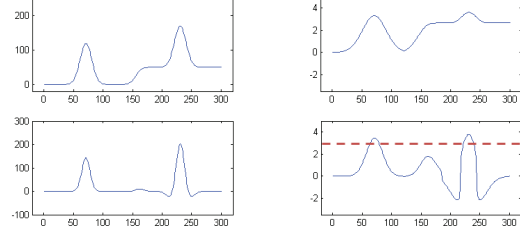


**Fig. 3.** Contrast Modification Example. (Top left is an example of two identical normal distributions with different background amplitudes. Bottom left is the contrast  $\psi(\cdot)$  of the sample. Top right is the result of performing gamma operation directly on the sample. Bottom right is the gamma corrected value  $I_c(\cdot)$  of the contrast  $\psi(\cdot)$ .)

$\{\alpha, \mu, \Sigma\} \in \Theta$  simultaneously, and it is solved by a SMEM algorithm which is an extension of the EM algorithm. In conventional applications of the EM algorithm, a mixture density is fit to clusters of sample points [7]. In EM shape modeling presented here, the measured frequency of realization of a random variable  $x$  is now equivalent to the normalized image intensity at pixel site  $(h, k)$ . Accordingly, the update equations for estimating the parameters of the  $m^{th}$  Gaussian component in the  $(i + 1)^{th}$  iteration of EM shape modeling, are modified as follows.

$$\begin{aligned} w_m(x_n) &= \frac{\alpha_m^i N_m(x_n | \theta_m^i) I_{norm}(x_n)}{\sum_{m=1}^M \alpha_m^i N_m(x_n | \theta_m^i)} \\ \alpha_m^{i+1} &= \frac{1}{N} \sum_{n=1}^N w_m(x_n) \\ \mu_m^{i+1} &= \frac{\sum_{n=1}^N x_n w_m(x_n)}{\sum_{n=1}^N w_m(x_n)} \\ \Sigma_m^{i+1} &= \frac{\sum_{n=1}^N w_m(x_n) (x_n - \mu_m^{i+1})(x_n - \mu_m^{i+1})^T}{\sum_{n=1}^N w_m(x_n)} \quad (1) \end{aligned}$$

Where  $w_m(x_n)$  is the hidden parameter which indicates the local mixing weight of the  $m^{th}$  component at the pixel site  $x_n$ . Their key modification is the use of  $I_{norm}(x_n)$  which is the normalized intensity value at pixel  $x_n$  and defined as

$$I_{norm}(x) = \frac{I(x)}{\sum_{n=1}^N I(x_n)} \quad (2)$$

**Initialization:** The process begins by initializing the number of mixture components  $M^0$  and the distribution parameters  $\{\alpha^0, \mu^0, \Sigma^0\} \in \Theta^0$  of the Gaussian components. The initial number  $M^0$  is defined by the number of local maxima in the intensity profile of the spot. The initial mixing weights  $\alpha^0$  are assigned as  $\frac{1}{M}$  and initial means  $\mu^0$  are the positions of the local maxima. The initial covariance of each component is estimated using the pixels inside a circle centered at its initial mean  $\mu^0$  with radius equal to the shortest distance between  $\mu^0$  and the boundary of the spot.

### 3.1. Split-and-merge operation

According to Eq.(1), the number  $M$  is not changed during the EM process. This means the amount of mixture components is defined by the number of maxima in the intensity profile

of the spots. When the protein particles are too close to each other, the shape could have only one maximum, or conversely, a spot may have more maxima than the actual proteins due to noise. In order to alter  $M$  and estimate the number of Gaussian components for the actual spot shape, a SMEM algorithm [8] is employed with split and merge steps as follows.

**Merge step:** This step proposes the creation of a new component  $k$  from two of the current mixture components  $i$  and  $j$ . The new parameters of  $k$  are estimated by the merge method defined as follows

$$\begin{aligned}\alpha_k &= \alpha_i + \alpha_j \\ \mu_k &= \frac{\alpha_i}{\alpha_k} \mu_i + \frac{\alpha_j}{\alpha_k} \mu_j \\ \Sigma_k &= \frac{1}{\alpha_k} (\alpha_i \Sigma_i + \alpha_i \mu_i \mu_i^T + \alpha_j \Sigma_j + \alpha_j \mu_j \mu_j^T) - \mu_k \mu_k^T\end{aligned}\quad (3)$$

**Split step:** The split operation is the reverse merge, that splits a current mixture component  $k$  into two new components  $i$  and  $j$ . Significantly, this manipulation is an under determined estimation as the new parameters being estimated (unknowns) are more than the present parameters (knowns). The fundamental problem is that the split directions and the split displacements of the new means  $\mu_i$  and  $\mu_j$  are undefined. While the covariance  $\Sigma_k$  is a symmetric positive definite matrix, it can be decomposed to  $A_k A_k^T$  using Cholesky decomposition. And a random column  $a_t^{(k)}$  of the matrix  $A = [a_1^{(k)}, \dots, a_n^{(k)}]$  is chosen as the split direction in this work. The split distance is adjusted by a random variable  $\nu$ . Also, two more random variables  $\gamma$  and  $\beta$  are introduced for the split of mixing weight  $\alpha_k$  and covariance  $\Sigma_k$  respectively. Moreover, the adopted split method should be guaranteed that the output parameters do not affect the current parameters of the remaining components. This means the present and new parameters should obey Eq.(3). According to [8], the split method is defined as

$$\begin{aligned}\gamma, \nu, \beta &\in (0, 1) \\ \left\{ \begin{array}{l} \alpha_i = \alpha_k \gamma \\ \mu_i = \mu_k - \sqrt{\frac{\alpha_j}{\alpha_i}} \nu a_t^k \\ A_i = A_k \text{diag} \left\{ \sqrt{\frac{\alpha_j}{\alpha_i}}, \dots, \sqrt{\beta(1-\nu^2) \frac{\alpha_k}{\alpha_i}}, \dots, \sqrt{\frac{\alpha_j}{\alpha_i}} \right\} \\ \Sigma_i = A_i A_i^T \end{array} \right. \\ \left\{ \begin{array}{l} \alpha_j = \alpha_k (1 - \gamma) \\ \mu_j = \mu_k + \sqrt{\frac{\alpha_i}{\alpha_j}} \nu a_t^k \\ A_j = A_k \text{diag} \left\{ \sqrt{\frac{\alpha_i}{\alpha_j}}, \dots, \sqrt{(1-\beta)(1-\nu^2) \frac{\alpha_k}{\alpha_j}}, \dots, \sqrt{\frac{\alpha_i}{\alpha_j}} \right\} \\ \Sigma_j = A_j A_j^T \end{array} \right.\end{aligned}\quad (4)$$

**Split-merge criteria** Since there are many components in the modeling process, reasonable criteria for ordering the mixture components are essential for the split and merge operations respectively. Although the merge and split steps are directly derived from [8], a novel split-merge step is needed here. As the shape modeling is a matching process, there is estimation error  $E$  between the estimated model  $I_{EM}$  and the target shape  $I_{norm}$ , where

$$E = I_{EM} - I_{norm}\quad (5)$$

In order to choose the ‘worst matched’ component and the ‘worst matched pair’ components, an error distribution is introduced for each component. The error distribution  $E_m(x_n)$

is the estimation error caused by the  $m^{th}$  component at pixel site  $x_n$  and expressed as

$$E_m(x_n) = w_m(x_n) E(x_n).\quad (6)$$

Therefore, the ‘worst matched’ component  $m_{split}$  being split is selected by

$$m_{split} = \arg \max_m \left( \sum_{n=1}^N |E_m(x_n)| \right)\quad (7)$$

We define the merge pair  $m_{merge}(i, j)$  by the component  $i$  with the smallest  $\alpha$  and the component  $j$  with the highest sum of error product with  $i$  over the modeled patch, as follows

$$\begin{aligned}m_{merge}(i) &= \arg \min_i (\alpha_i) \\ m_{merge}(j) &= \arg \max_j \left( \sum_{n=1}^N |E_i(x_n)| |E_j(x_n)| \right) \quad (i \neq j)\end{aligned}\quad (8)$$

### Final Iterative Algorithm

The overall SMEM modeling process is as follows

1. Run EM estimation with initial parameters  $\Theta^0$  as discussed to yield parameters  $\Theta_i$ .
2. Perform a split-step on  $\Theta_i$  and run EM with this split output to yield parameters  $\Theta_s$ .
3. Perform a merge-step on  $\Theta_s$  and run EM with this merge output to yield parameters  $\Theta_m$ .
4. Select  $\Theta_m$  if the error is lower than the error with  $\Theta_i$ , otherwise choose  $\Theta_s$ .
5. Iteratively repeat steps 2,3&4 until convergence, i.e the rate of change of the sum of estimation error is less than a certain value (it is set to 0.2 in our experiment).

## 4. RESULTS AND DISCUSSION

The SMEM modeling algorithms is tested with synthetic samples, where each testing sample is a Gaussian mixture model with  $M$  components. The results in Fig.4 shows that the SMEM algorithm is a powerful modeling tool. Although the performance is slightly decreased for larger number of  $M$ , the estimated shapes are still satisfactory since the average estimation error  $\mathbb{E}$  is negligibly small.

$M$	$N$ (%)	$e_\alpha$	$\frac{e_\alpha}{\alpha}$ (%)	$e_\mu$	$e_\sigma$	$e_\rho$	$\mathbb{E}$ (%)
2	100	0.0000	0.00	0	0.0000	0.0000	0.00
3	99	0.0013	0.37	0.02	0.0075	0.0012	0.23
4	98	0.0011	0.44	0.04	0.0120	0.0020	0.36
5	96	0.0023	1.20	0.11	0.0197	0.0047	0.62
6	87	0.0026	1.64	0.11	0.0293	0.0058	1.32
7	89	0.0037	2.63	0.23	0.0502	0.0106	1.62
8	80	0.0057	4.53	0.55	0.1019	0.0201	2.62

**Fig. 4.** Ground-truth evaluation (*The algorithm is tested using estimation on spots created from synthetic Gaussian mixtures of order  $M$ . For each  $M$  we test 100 trials of randomly sampled Gaussian components.  $N$  is the amount (%) of trials in which the estimated  $M$  is equal to the true  $M$  after SMEM modeling.  $\{e_\alpha, e_\mu, e_\sigma, e_\rho\}$  are the average absolute errors of the estimated parameters  $\alpha, \mu$  (in pixel),  $[\sigma_h, \sigma_k]$  (2~6 pixels) and  $\rho$ .  $\mathbb{E}$  is the average sum of estimation error over all trials.*)

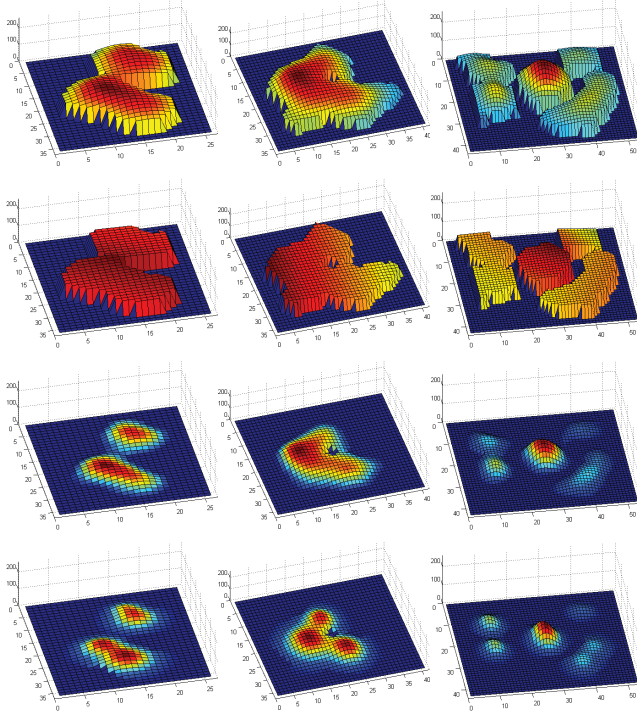


**Fig. 5.** Modeling results (The first row shows the extracted spot patches. The second row shows the estimated local background. The third row shows the normalized and background subtracted spot patches. The last row shows the corresponding model estimations.)

For real data, as shown in Fig.5, the SMEM modeling algorithm is successful in characterizing spot shapes analytically. Even when protein particles are clustered and yield merged spot shapes, the algorithm can generate reliable estimation of the sizes and positions of particles in those spots.

However, since the split method employs random splits, the model parameters may converge to different values in EM operation when repeating the process. This means the modeling estimation is not repeatable. The current approach is to perform multiple split operations (20 in our experiment) simultaneously with the same  $\Theta_i$  in step 2 of the algorithm and to choose the one with least estimation error as the output  $\Theta_s$ . To improve the efficiency, a possible approach is using the error distribution of the ‘worst matched’ component to estimate the positions of new components instead of the random variable dependence.

**Co-localization analysis:** After shape modeling, the user selects appropriate particles that lie within suitable ranges of brightness ( $I(\vec{\mu})$ ) and sizes ( $\sigma$ ) and local background ( $B(\vec{\mu})$ ). The particles that satisfy these requirements are then used for co-localization analysis. We find the ‘nearest neighbor’ of each particle on one image (‘red’) from the other image (‘green’), and measure the distance  $R$  between their means ( $\vec{\mu}^{red}$  and  $\vec{\mu}^{green}$ ). The co-localization is then defined by the ratio  $\frac{R}{\sigma_r + \sigma_g}$ . Where  $\sigma_r$  ( $\sigma_g$ ) is the mean standard deviation  $\frac{\sigma_h + \sigma_k}{2}$  of a particle model, derived from  $\Sigma =$

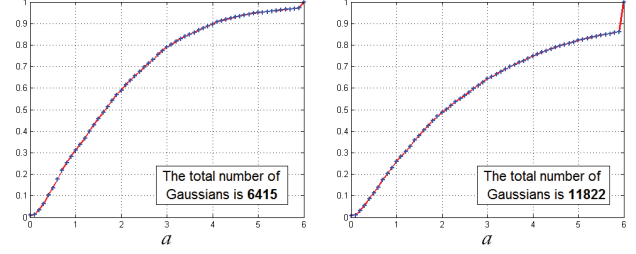


**Fig. 6.** Co-localization analysis (The cumulative plot on the left shows the ratio  $a = \frac{R}{\sigma_r + \sigma_g}$  versus the number of particles (in percentage) for the proteins in ‘red’ image with ‘nearest neighbor’ in ‘green’ image. The right plot is for the proteins in ‘green’ image.)

$\begin{bmatrix} \sigma_h^2 & \rho\sigma_h\sigma_k \\ \rho\sigma_h\sigma_k & \sigma_k^2 \end{bmatrix}$ . Hence  $\sigma_r$  ( $\sigma_g$ ) can be considered as radius of the particle and the cumulative plot (Fig.6) therefore shows the % of particles in one image that are colocalized with their ‘nearest neighbor’ in the other image within some distance.

The modeling algorithm is robust in automatically estimating the amount, positions and sizes of protein particles in the spots with varying shapes. In our experiment, the analyzed results confirmed that Me31B co-localized much more efficient with Dcp1, Pcm and Staufen in cell bodies than it did at synaptic areas [9]. For example, based on using 200nm (10 pixels) cut-off for perfect co-localization, Me31B showed 58% co-localization with Dcp1 in soma, but only 7% at the synapse. Thus the data indicate that, in adult *Drosophila* brain, the Me31B particles in cell bodies are different from the particles in synaptic areas.

## 5. REFERENCES

- [1] I. Smal, M. Loog, W. Niessen, and E. Meijering, “Quantitative comparison of spot detection methods in live-cell fluorescence microscopy imaging”, *IEEE Transaction on Medical Imaging*, vol. 29, no. 2, pp. 282–301, 2010.
- [2] J.-C. Olivo-Marin, “Extraction of spots in biological images using multiscale products”, *Pattern Recognition*, vol. 35, no. 9, pp. 1989–1996, 2002.
- [3] B. Zhang, M. J. Starck, and J.-C. Olivo-Marin, “Multiscale variance-stabilizing transform for mixed-poisson-gaussian processes and its applications in bioimaging”, *IEEE International Conference on Image Processing (ICIP)*, 2007.
- [4] S. Jiang, X. Zhou, T. Kirchhausen, and S. T. C. Wong, “Detection of molecular particles in live cells via machine learning”, *Cytometry Part A*, vol. 71, no. 8, pp. 563–375, 2007.
- [5] I. Smal, W. Niessen, and E. Meijering, “A new detection scheme for multiple object tracking in fluorescence microscopy by joint probabilistic data association filtering”, *IEEE International Symposium on Biomedical Imaging (ISBI)*, 2008.
- [6] A.-O. Boudraa and E.-H. S. Diop, “Image contrast enhancement based on 2d teager-kaiser operator”, *IEEE International Conference on Image Processing (ICIP)*, pp. 3180–3183, 2008.
- [7] A. P. Dempster, N. M. Laird, and D. B. Rubin, “Maximum likelihood from incomplete data via the em algorithm”, *Journal of the Royal Statistical Society. Series B (Methodological)*, vol. 39, no. 1, pp. 1–38, 1977.
- [8] Z. Zhang, C. Chen, J. Sun, and K. L. Chan, “Em algorithms for gaussian mixtures with split-and-merge operation”, *Pattern Recognition*, vol. 36, no. 9, pp. 1973–1983, 2003.
- [9] S. A. Barbee, P. S. Estes, A.-M. Cziko, J. Hillebrand, R. A. Luedeman, J. M. Collier, N. Johnson, I. C. Howlett, C. Geng, R. Ueda, A. H. Brand, S. F. Newbury, J. E. Wilhelm, R. B. Levine, A. Nakamura, R. Parker, and M. Ramaswami, “Staufen- and fmrp-containing neuronal rnp are structurally and functionally related to somatic p bodies”, *Neuron*, vol. 52, no. 6, pp. 997–1009, 2006.